VOL. 09 NO. 5,
AUGUST, 2025
E-ISSN 3027-1339
P-ISSN 3026-8257

African Scholar Publications & Research International
www.africanscholarpub.com

Journal of Systematic, Evaluation and Diversity Engr. (JSEDE)

Energy Distribution Model Using Modified Hylleraas potential (MHsP) Based Non-Relativistic Schrödinger Equation

P. J. Manga[1]; R. O. Amusat[2]; Ocheni, A.U. U.[3]; Amina A. Dibal[4]; Mustapha M.K.[5]; Akoh A. Mary[6]

[1-4]Department of Physics, University of Maiduguri, Borno State – Nigeria. [5]Department of Technical Education Ramat Polytechnic, Maiduguri, Borno State – Nigeria. [6]Government Girls Day Secondary School Games – Village, Bauchi State – Nigeria.

DOI: https://doi.org/10.70382/ajsede.v9i5.019

Abstract

Solving the Schrödinger equation for systems with multiple particles is particularly challenging due to the intricacies of inter-particle interactions. In this study, we utilize the Modified Hylleraas Potential (MHsP), which provides a more precise depiction of these interactions. Incorporating this refined potential into the non-relativistic Schrödinger equation enables a deeper insight into atomic and molecular structures, as well as their dynamic behaviour. The study further explores how changes in the dimensionless potential parameters (λ, V_0 and V_1) influence the predicted energy spectrum. It was found that for V_1values between 0.01 and 0.03, the molecular interactions intensify, leading to a higher energy spectrum. However, this effect diminishes at $V_1 = 0.04$ when evaluated against V_0. Similarly, a significant energy spectrum is noted for λ values ranging from 1 to 3, but this decreases at $\lambda = 4$ when analysed in conjunction with V_1 under varying V_0. Results derived using Maxwell-Boltzmann, Fermi-Dirac, and Boltzmann statistical models indicate that at lower values of the temperature parameter (β), intermolecular interactions are stronger. Conversely, higher β values correspond to weaker interactions and a lower energy spectrum. Moreover, plotting the energy spectrum against β under different dimensionless parameters shows that energy increases as these parameters rise. The behaviour of the partition function mirrors these trends—initially increasing at low β values and decreasing at higher temperatures, thereby also impacting molecular interactions.

Keywords: Partition Function, Non-Relativistic Schrödinger Equation, Potential Parameters and Hylleraas Potential

Introduction

Accurately comprehending atomic and molecular structures relies on analysing energy distribution within quantum systems (Manga et al., 2023). This analysis plays a vital role in quantum mechanics and is closely associated with the non-relativistic Schrödinger equation, which analytically describes the behaviours of particles at the atomic level (Manga et al., 2025A). Nonetheless, finding exact solutions to the Schrödinger equation for systems involving multiple particles remains difficult, mainly due to the intricate effects of inter-particle interactions, especially electron correlation (Manga et al., 2025A).

To address this, potential models such as the Modified Hylleraas Potential (MHsP) have been developed. Originally introduced to better account for the electron-electron repulsion in the helium atom, the Modified Hylleraas Potential (MHsP) incorporates correlation effects that are often neglected in simpler models (Manga et al., 2025B). In this work, we propose a modified form of the Hylleraas Potential (HsP) tailored for enhanced applicability and physical realism in few-body quantum systems. Similarly, energy spectrum of a system is determined by solving the Schrödinger equation using a specific interaction potential (Alrebdi et al., 2024). The nature of the interactions between particles in the system dictates the type of potential applied. Various potential forms exist, such as the harmonic, Coulomb, Kratzer potential (Alrebdi et al., 2024), Cornell potential (Abushady & Khokha, 2023), perturbed Yukawa potential (Manga et al., 2023), pseudo-harmonic potential (Ikot et al., 2021), Morse potential (Ikot et al., 2021), and the Deng–Fan–Eckart potential, among others. Some algebraic sums of these potentials have been carried out to obtain their approximate and exact solutions by many researchers but in turned to be in vain due to ambiguity parameters (Abu-Shady & Khokha, 2023).

The modified Hylleraas potential (MHsP) is relatively underexplored and presents an opportunity to expand the catalogue of solvable potentials. This study aims to solve the Schrodinger equation (SE) for MHP and subject it four different energy distribution models such as Maxwell-Boltzmann distribution, Fermi Dirac distribution, Bose-Einstein Distribution and Boltzmann Distribution. Over time, a wide range of analytical and numerical methods have been developed for solving the Schrödinger equation (SE), many yielding similar results. Thermodynamics, which connects macroscopic observations to microscopic behaviour using statistical mechanics, has also been a focus in quantum systems, with several researchers analysing thermal properties under various potentials (Abu-Shady & Khokha, 2023).

Our method presents an energy distribution model that partitions the system's total energy using the revised potential. This division enables the examination of how various

regions of the potential contribute to the overall energy states. Utilizing the non-relativistic Schrödinger equation within this modified potential framework, we obtain analytical or semi-analytical expressions for the energy eigenvalues and energy distribution model based on partition function.

Hylleraas plus Yukawa Potential (Modified Hylleraas Potential (MHsP))

The wave equation solutions in relativistic and nonrelativistic of quantum mechanical system (QMS) have presently been becoming centre of great interest (Abu-Shady & Khokha, 2023). Many researchers for decade have made a lot of effort in evaluating their energy and that of their corresponding wave functions. Furthermore, this arises as a result of vast application in studying several physical systems of interest. Modified Hylleraas potential (MHsP) is one of the potentials can be solved exactly seen the buttressed (Abu-Shady & Khokha, 2023). The Hylleraas potential (HsP) was proposed as an intermolecular potential and it was found to be fit for many vibrational energy studies of diatomic molecules. Ikot et al. (2021), pointed out that Hylleraas potential (HP) is a special case of multiparameter exponential because since Hylleraas introduce it, no much work been reported on it bound state solution in both relativistic and non relativistic from. On the same note, we proposed a modified of its kind called Hylleraas plus Yukawa Potential (Modified Hylleraas Potential (MHsP)) for the designated studies (Abu-Shady & Khokha, 2023).

$$V(r) = \frac{V_0}{b}\frac{a- e^{-2\delta r}}{1- e^{-2\delta r}} + \frac{V_1\, e^{-2\delta r}}{r} \quad \ldots (1)$$

Where δ is the screening parameter. Ever since then, several adjustments have been proposed but in the case of our study we focus on equation (1). Note, since hylleraas introduce this potential that very minute researcher has started using it.

Radial Solution of the Schrödinger equation based on Hylleraas plus Yukawa potential (MHsP).

The motion of a particle in a radial part of a spherical symmetric with potential $V(r)$ is given as (Ettah, 2021).

$$\frac{d^2R}{dr^2} + \left[\frac{2\mu}{\hbar^2}\big(E - V(r)\big) - \frac{\delta}{r^2}\right]R(r) = 0 \quad \ldots (2)$$

Where $\eth = \tau(\tau+1)$ equation (2) becomes

$$\frac{d^2R}{dr^2} + \left[\frac{2\mu}{\hbar^2}\big(E - V(r)\big) - \frac{\tau(\tau+1)}{r^2}\right]R(r) = 0 \quad \ldots (3)$$

Equation (3) can not be solved analytically for $\tau \neq 0$ due to the ambiguity parameters as centrifugal term, we apply the Greene and Aldrich approximation scheme to the centrifugal term as follows.

$$\frac{1}{r^2} = \frac{4\delta^2 e^{-2\delta r}}{\left(1-e^{-2\delta r}\right)^2} \quad = \frac{1}{r} = \frac{2\delta e^{-2\delta r}}{(1-e^{-2\delta r})} \qquad \ldots (4)$$

It is convenient to point out for a given short-range potential, equation (4) found to be good approximation to $\frac{1}{r^2}$, which implies that it is not a good approximation to the centrifugal barrier in the condition of larger screening parameter δ. This approximation said to be valid for certain value of $\delta r \ll 1$. Thus, by substituting equation (1) into equation (2) then later apply Greene and Aldrich approximation as it is in equation (4), we have.

$$\frac{d^2R}{dr^2} + \left[\frac{2\mu}{\hbar^2}\left(E - \frac{V_0}{b}\frac{a- e^{-2\delta r}}{1- e^{-2\delta r}} + \frac{2\delta V_1\, e^{-4\delta r}}{(1-e^{-2\delta r})}\right) - \frac{4\delta^2 e^{-2\delta r}\tau(\tau+1)}{\left(1-e^{-2\delta r}\right)^2}\right] R(r) = 0 \qquad \ldots (5)$$

We transform the coordinate of equation one as follows

$$\frac{d^2}{dr^2} + \frac{1}{u}\frac{d}{dr} + \frac{1}{u^2(1-u)^2}\left(\frac{\mu E}{2\delta^2\hbar^2} - \frac{\mu E u}{\delta^2\hbar^2} + \frac{\mu E u^2}{2\delta^2\hbar^2} - \frac{V_0 a}{4\delta^2 b} + \frac{V_0 u}{4\delta^2 b} + \frac{V_0 a u}{4\delta^2 b} - \frac{V_0 u^2}{4\delta^2 b} - \frac{V_1 u}{\delta} + \frac{V_1 u^2}{\delta} - u\tau^2 - u\tau\right) R(u) = 0 \qquad \ldots (6)$$

In other to obtain a hypergeometric solution of equation (6) we transform it as follows (Dong, 2000).

$$\frac{d^2}{dr^2} + \frac{1(1-u)}{u(1-u)}\frac{d}{dr} + \frac{1}{u^2(1-u)^2}\{(-A - C + D)u^2 + (-2A + C + B - D - \tau^2 - \tau)u - A - B\} \qquad \ldots (7)$$

Where following dimensionless constant was used as it is in equation (7)

$$\frac{\mu E}{2\delta^2\hbar^2} = E_{n,l} = A,\ B = \frac{V_0 a}{4\delta^2 b},\ C = \frac{V_0}{4\delta^2 b},\ D = \frac{V_1}{\delta}, \qquad \ldots (8)$$

Equation (7) has satisfied the hypergeometric function of the form .

$$\psi_n'' + \frac{\chi_1 - \chi_2 s}{s(1-\chi_3 s)}\psi' + \frac{1}{s^2(1-\chi_3 s)^2}[-\mathfrak{T}_1 s^2 + \mathfrak{T}_2 s - \mathfrak{T}_3]\psi(s) = 0 \qquad \ldots (9)$$

Comparing equation (7) and (8) we have

$$\mathfrak{T}_1 = -A - C + D;\ \mathfrak{T}_2 = -2A + C + B - D - \tau^2 - \tau;\ \mathfrak{T}_3 = -A - B \qquad \ldots (10)$$

The gauss hypergeometric equation can be obtained as

$$\gamma = \frac{1}{2}\left((1-\delta_1) \pm \sqrt{(1-\delta_1)^2 + 4\mathfrak{T}_3}\right) \qquad \ldots (11)$$

$$\gamma^2 = -A - B \qquad \ldots (12)$$

The coiling velocity based on Nikiforov Uvarov Functional Analysis method given as (Manga et al., 2025C).

$$\omega = \frac{1}{2\delta_3}\left((\delta_3 + \delta_1\delta_3 - \delta_2) \pm \sqrt{(\delta_3 + \delta_1\delta_3 - \delta_2)^2 + 4\left(\frac{\mathfrak{T}_1}{\delta_3} + \delta_2\mathfrak{T}_3 - \mathfrak{T}_2\right)}\right) \quad \text{... (13)}$$

$$\omega = \frac{1}{2}\left(1 + \sqrt{1 + 4(-2C + 2D + \tau^2 + \tau - 2B)}\right) \quad \text{... (14)}$$

After equating equation (12) by equation (14) we deduced our bound state energy eigenvalue equation as;

$$E_{n,l} = B + \left(\frac{-C+D+B-(\omega+n)^2}{2(v+n)}\right)^2 \quad \text{... (15)}$$

Equation (15) can be rewrite by substituting the dimensionless constant as given in equation (8), we have

$$E_{n,\tau} = \frac{2\delta^2\hbar^2}{\mu}\frac{V_0 a}{4\delta^2 b} + \frac{2\delta^2\hbar^2}{\mu}\left(\frac{-\frac{V_0}{4\delta^2 b}+\frac{V_1}{\delta}+\frac{V_0 a}{4\delta^2 b}-(\omega+n)^2}{2(\omega+n)}\right)^2 \quad \text{... (16)}$$

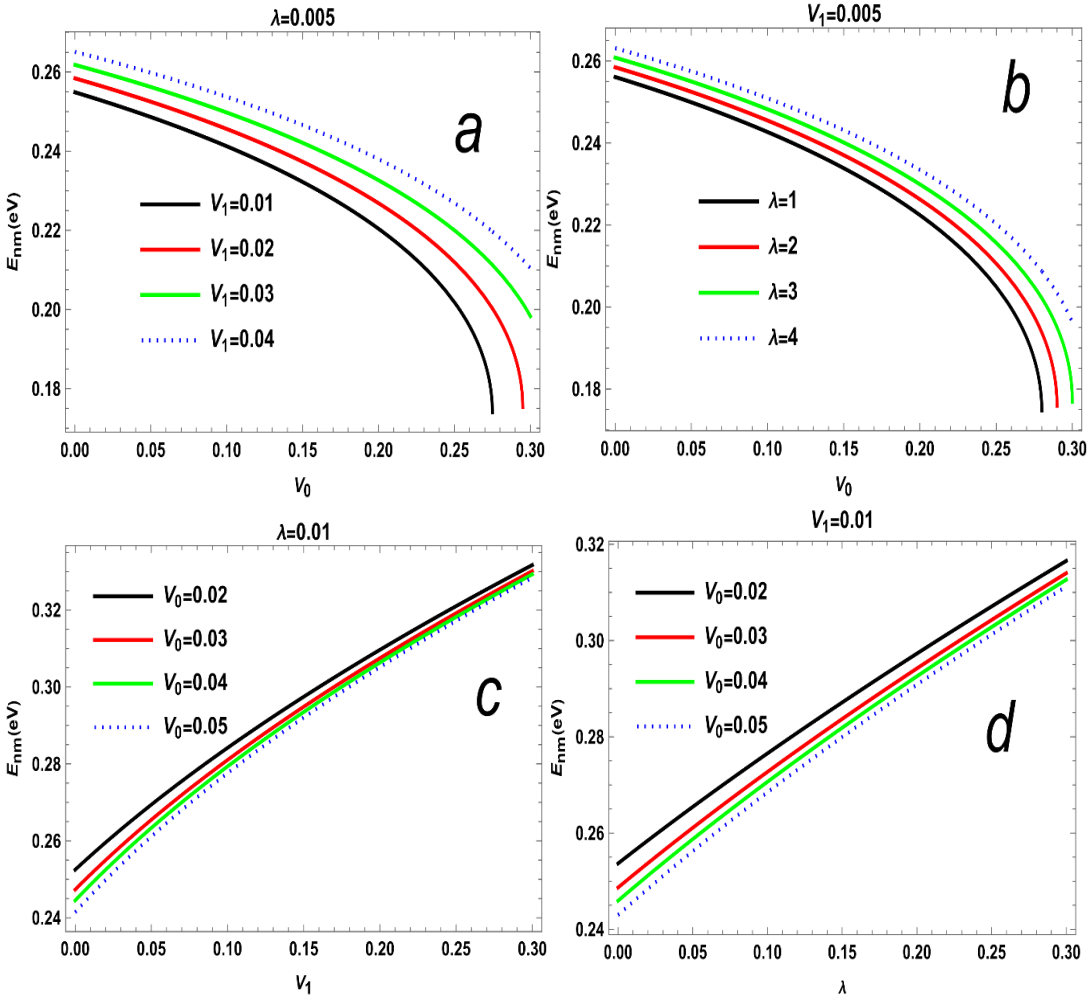


Figure 1: Computed energy spectrum under varying potential parameters.

Figure 1 presents the computed energy spectrum obtained from the non-relativistic Schrödinger equation under different potential parameter settings. As illustrated in plots (a), (b), (c), and (d), plots (a) and (b) indicate that the energy spectrum is higher when V_0 and V_1 are small, with variations in λ and V_1. As these potential parameters increase, the energy spectrum decreases. A similar trend is observed in plots (c) and (d), demonstrating that the potential parameters significantly influence the energy spectrum by increasing the particles' energy eigenvalues.

Maxwell – Boltzmann Distribution

In nonrelativistic systems, the Maxwell-Boltzmann distribution is essential for characterizing the behaviour of particles, particularly in conditions involving high temperatures or low particle densities, such as in an ideal gas. Additionally, it provides a framework for understanding how kinetic energy is distributed among individual particles within the system (Umirzakov, 2019).

$$f(E) = k_\beta e^{-(E/k_\beta T)} \quad \ldots (17)$$

where β is a temperature parameter given as $\beta = \frac{1}{k_\beta T}$

$$f(E) = e^{-\frac{4K_1 + \frac{K_3(P^4 - K_2(2P^2 + K_3))}{P^2}}{4\beta}} K_\beta \quad \ldots (18)$$

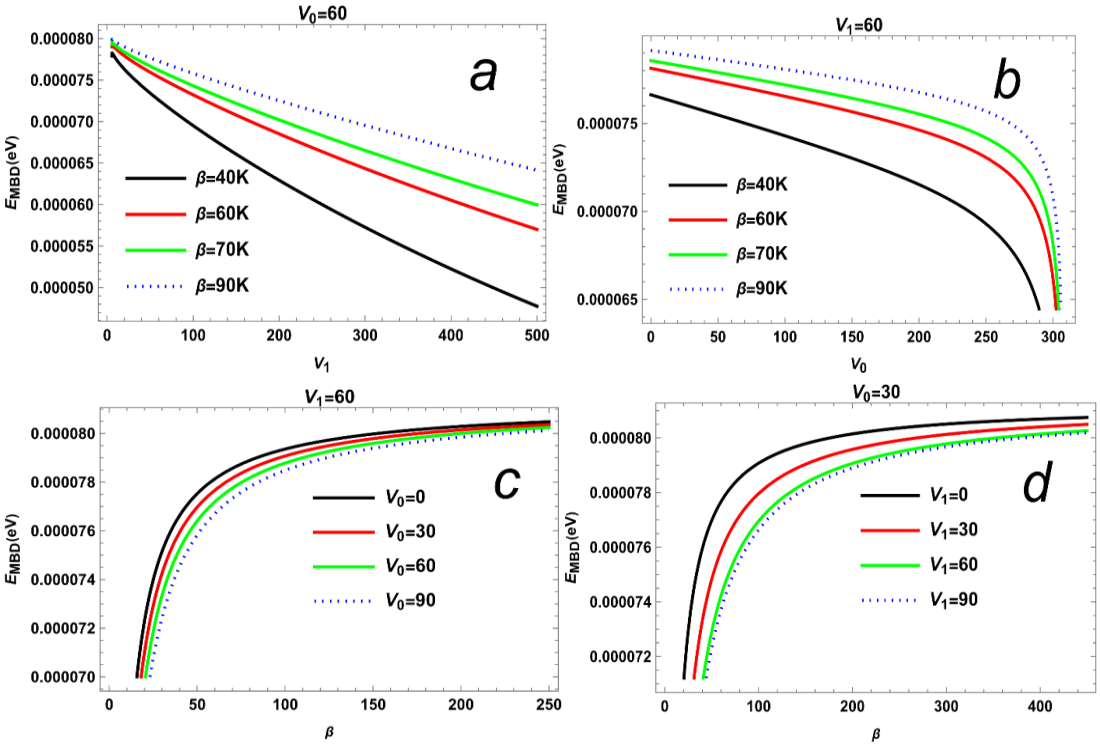


Figure 2: Computed energy spectrum based on maxwell boltzmann distribution under varying potential parameters.

Figure 2 shows four subplots (a, b, c, d) illustrating how the computed energy spectrum (E_{MBD}) based on Maxwell-Boltzmann distribution under varying the potential parameters and temperature-related parameters affected the estimated energy spectrum. Plot (a) is the computed energy spectrum which decreases monotonically as V_1 increases. It is also show in plot (a) that the higher (β) lower temperature results into higher energy spectrum. Plot (b) show a similar effect as seen in plot (a) the energy computed decreases as V_0 increases. Plot (c) as shown, the energy spectrum increases as temperature increases. Plot (d) the effect of the potential parameter showing a supressed in the energy spectrum by increase V_1. The nature of Maxwell-Boltzmann influence, as expected, at higher temperatures, the average energy spreads more, reducing the likelihood of finding particles at lower energy states.

Fermi – Dirac Distribution

In nonrelativistic systems, the Fermi-Dirac distribution applies to particles that are typically identical and indistinguishable, referred to as fermions. These particles, such as electrons, possess half-integer spin. According to the Pauli exclusion principle, no two fermions can occupy the same quantum state simultaneously, which imposes a fundamental restriction on their behaviour in a system (Manga et al., 2025B).

$$F(E) = \frac{1}{e^{-(E-\mu/\beta)}} \quad \ldots (19)$$

These can rewrite as

$$f(E) = e^{-\frac{-\mu+\frac{1}{2}(2K_1-K_2K_3)+\frac{1}{4}(P^2K_3-\frac{K_2K_3^2}{P^2})}{\beta}} \quad \ldots (20)$$

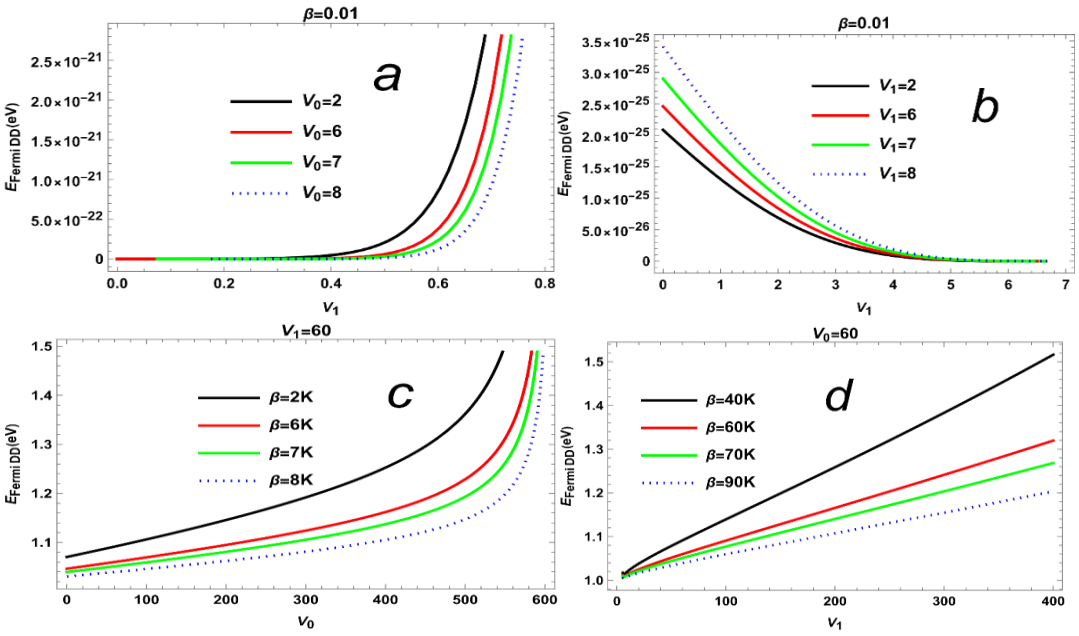


Figure 3: Computed energy spectrum based on fermi-dirac- distribution under varying potential parameters.

Figure 3 presents the computed energy spectrum derived from the Fermi-Dirac Distribution for different values of the potential parameters**.** In plot (a), the energy spectrum is shown as a function of V_1 at a fixed temperature parameter $\beta = 0.01K$. It is observed that as V_0increases, the energy spectrum also rises.

Plot (b) illustrates the energy spectrum versus V_0 while varying V_1. It reveals that for smaller values of V_1 (between 2 and 4), the energy spectrum remains high; however, at larger V_1 values, the energy spectrum shows a slight decrease. Similarly, plots (c) and (d) depict the relationship between the energy spectrum and the temperature parameter β. These plots indicate that higher temperatures correspond to higher energy spectra. Overall, the two plots confirm that the computed energy spectrum is significantly influenced by changes in the potential parameters within the framework of the Fermi-Dirac distribution.

Boltzmann Distribution

In nonrelativistic systems, the distribution function defines the probability that a particle will occupy a particular energy state or remain confined within a bound state. This probability is influenced by factors such as the energy of the state and the temperature of the system, and it provides a statistical description of how particles are distributed among available energy levels in equilibrium (Dong, 2000).

$$P(E) = \frac{e^{-(E/k_\beta T)}}{Z} \quad \ldots (21)$$

$$P(E) = \frac{2e^{\frac{1}{2}\sqrt{-\beta K_2}\sqrt{\beta K_2 K_3^2}-\frac{1}{2}\beta(-2K_1+K_2K_3)+\frac{\frac{1}{2}(-2K_1+K_2K_3)+\frac{1}{4}(-P^2K_3+\frac{K_2K_3^2}{P^2})}{\beta}}\sqrt{-\beta K_2}}{\sqrt{\pi}(1+e^{\sqrt{-\beta K_2}\sqrt{\beta K_2 K_3^2}}(-1+\mathrm{Erf}[\frac{P^2\sqrt{-\beta K_2}+\sqrt{\beta K_2 K_3^2}}{2P}])+\mathrm{Erf}[\frac{1}{2}P\sqrt{-\beta K_2}-\frac{\sqrt{\beta K_2 K_3^2}}{2P}])} \quad \ldots (22)$$

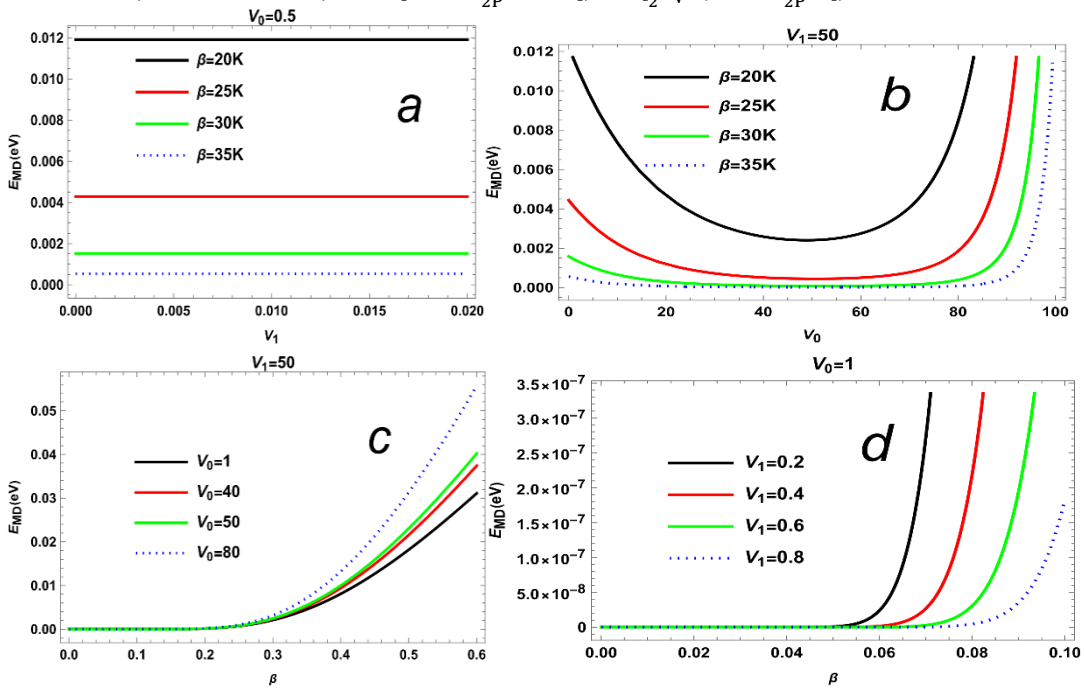


Figure 4: Computed energy spectrum based on Boltzmann distribution under varying potential parameters

Figure 4 presents the computed energy spectrum based on the Boltzmann distribution while varying the potential parameters, with behaviour similar to trends observed in the Maxwell distribution of particle energies. In plot (a), with $V_0 = 0.5$, the energy spectrum shows a nearly linear increase with temperature, resembling the linear dependence seen in the low-energy regime of the Maxwell distribution. Plot (b), at $V_1 = 50$, indicates that at low temperatures, the energy spectrum is initially high, decreases, and then rises again with increasing temperature, reflecting the shift and broadening of energy distribution typically described by the Maxwell distribution as temperature rises. Similarly, plots (c) and (d) demonstrate that as temperature increases, the computed energy spectrum also increases, consistent with the behaviour predicted by both Boltzmann and Maxwell statistics when potential parameters V_0 and V_1 are varied.

Bose – Einstein Distribution

The Bose-Einstein distribution describes how identical bosons, which are particles with integer spin, are statistically distributed across various energy states when the system is in equilibrium. This distribution plays a crucial role in quantum statistics and is particularly significant in phenomena like Bose-Einstein condensation, where a group of bosons occupy the same quantum state at very low temperatures (Dong, 2000).

$$B(E) = \frac{1}{e^{-(E-\mu/\beta)-1}} \quad \ldots (23)$$

$$B(E) = \frac{1}{-1+e^{\frac{-\mu+\frac{1}{2}(2K_1-K_2K_3)+\frac{1}{4}(P^2K_3-\frac{K_2K_3^2}{P^2})}{\beta}}} \quad \ldots (24)$$

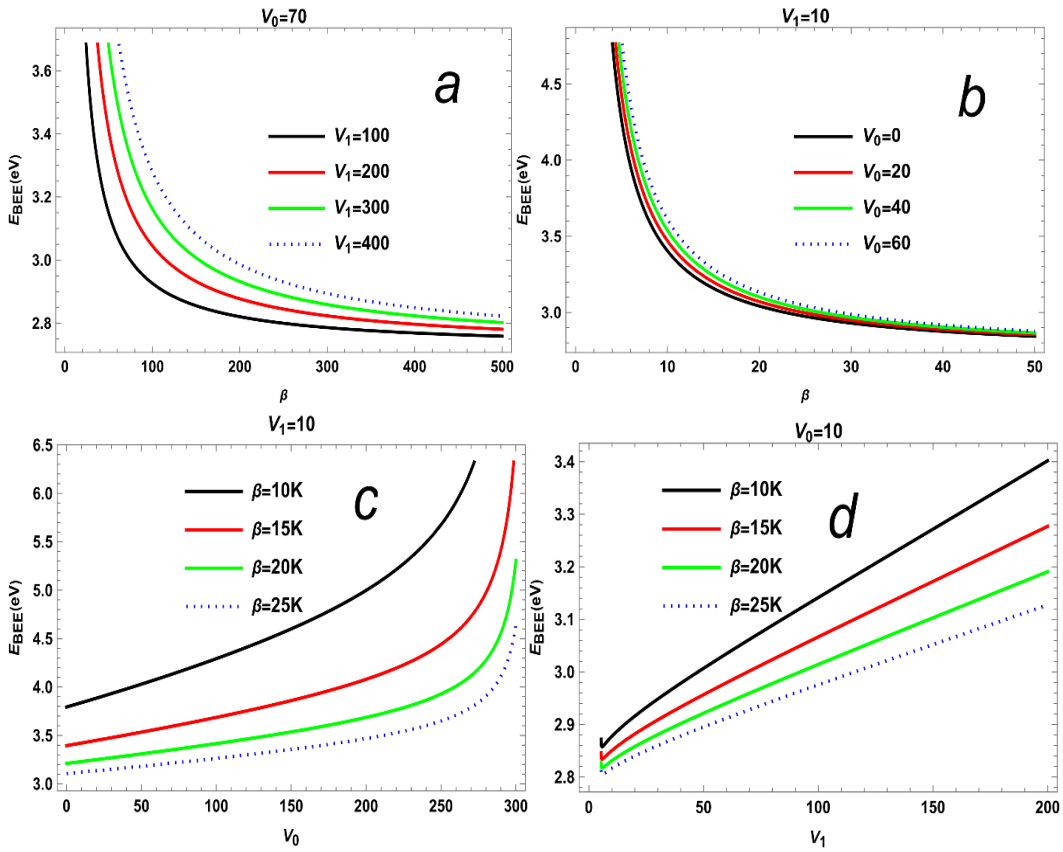


Figure 5: Computed energy spectrum based on Bose-einstein distribution under varying potential parameter.

Based on the Bose-Einstein distribution, Figure 5 presents the computed energy spectrum. The results indicate that for V_1 values between 100 and 200, the energy spectrum is relatively high but gradually decreases as V_1 increases from 200 to 400. Similarly, in plot (b), a high energy spectrum is observed when V_0 ranges from 0 to 30, followed by a decline as V_0 increases from 40 to 60. This trend mirrors that of plot (a), where lower values of V_0 and V_1 correspond to a higher energy spectrum, while higher values lead to a reduction. Plots (c) and (d) display the energy spectrum as functions of V_0 and V_1, respectively. It was observed that an increase in temperature results in a corresponding increase in the computed energy spectrum.

Thermodynamic properties

In this section, the thermodynamic characteristics corresponding to the proposed potential model are systematically derived. These quantities are obtained through the precise evaluation of the partition function, given by (Manga et al., 2025A)

$$Z(\beta) = \sum_{n=0}^{\lambda} e^{-\beta E_n} \quad \ldots (26)$$

where λ denotes the maximum vibrational quantum number, determined by solving $\frac{dE_n}{d_n} = 0$, $\beta = \frac{1}{KT}$. The parameter β is defined as $\beta = \frac{1}{KT}$, with k representing the Boltzmann constant and T the absolute temperature. In cases where the quantum number becomes sufficiently large, the summation over discrete states can be approximated by a continuous integral, as outlined in references (Manga et al., 2025A).

$$Z(\beta) = \int_0^{\lambda} e^{-\beta E_n}\, dn \qquad \ldots (27)$$

The energy equation can be represented under a partition function as follows.

$$ZZ = e^{-\frac{\beta}{2}(K_2K_3 - 2K_1)} \int_0^{\lambda} e^{-\frac{\beta}{4}\left(\frac{K_2K_3^2}{P^2} + K_2P^2\right)} dP \qquad \ldots (29)$$

ZZ=

$$\frac{e^{\frac{1}{2}(-2k1+k2k3)\beta - \frac{1}{2}\sqrt{-k2\beta}\sqrt{k2k3^2\beta}}\sqrt{\pi}\left(1+e^{\sqrt{-k2\beta}\sqrt{k2k3^2\beta}}\left(-1+\mathrm{Erf}\left[\frac{p^2\sqrt{-k2\beta}+\sqrt{k2k3^2\beta}}{2p}\right]\right)+\mathrm{Erf}\left[\frac{1}{2}p\sqrt{-k2\beta}-\frac{\sqrt{k2k3^2\beta}}{2p}\right]\right)}{2\sqrt{-k2\beta}}$$

... (30)

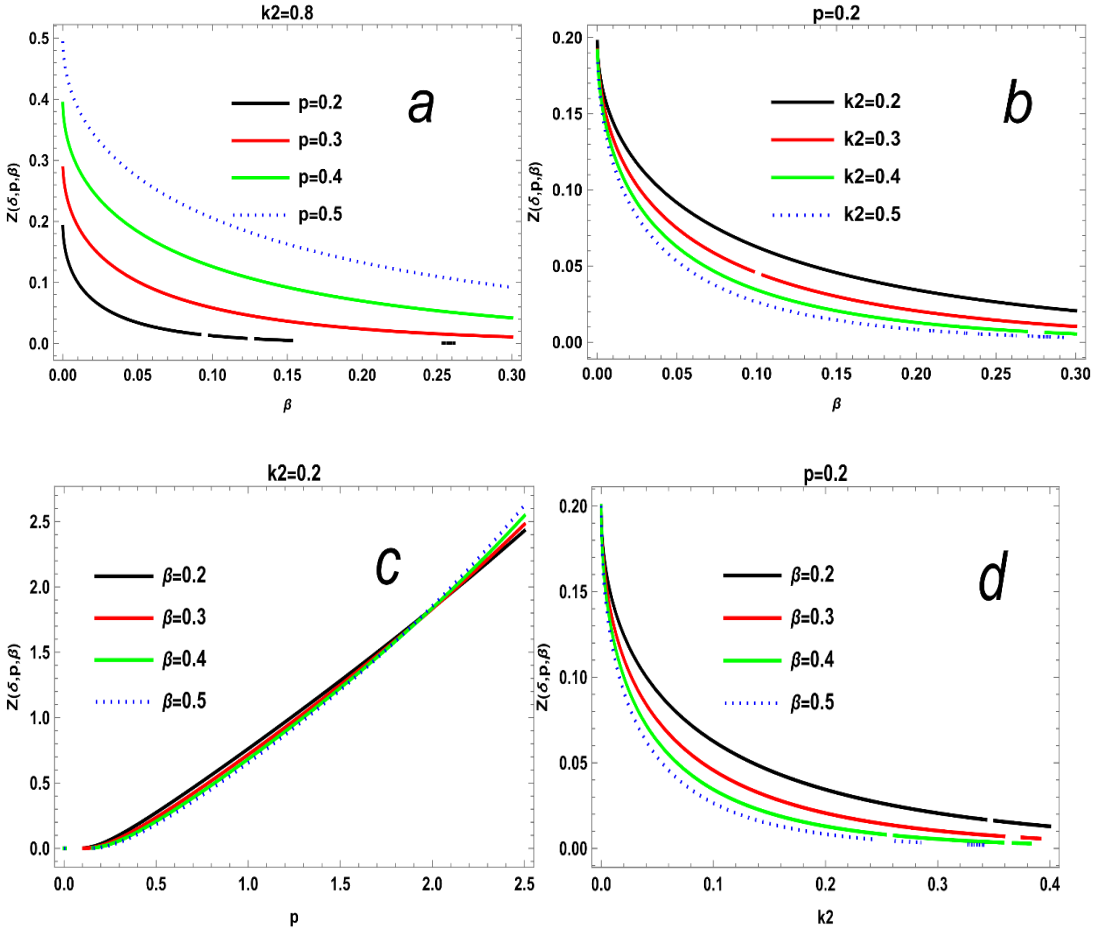


Figure 6: Computed partition function under varying potential parameters.

According to the principles of partition function theory, Figure 6 presents the variation of the partition function with respect to different potential parameters. In plot (a), for values of p ranging from 0.2 to 0.5, the partition function exhibits an overall increasing trend. However, a slight reduction is noticeable when p moves from 0.2 to 0.5, suggesting that the growth rate diminishes at higher p values within this range.

In plot (b), the partition function behaviour with respect to k2 is illustrated. It is observed that at lower values of k2 the partition function increases, indicating enhanced system stability. As k2 continues to increase, however, the partition function begins to decline, implying that stronger potential parameters may reduce the number of accessible microstates.

Plot (c) depicts the partition function as a function of p under varying temperatures. It is evident from the plot that as the temperature rises, the partition function correspondingly increases, demonstrating the direct relationship between thermal energy and the number of accessible states within the system.

Another plot (also labelled as plot (c)) shows the partition function plotted against k2 at different temperatures. Here, it is found that at low temperatures, the partition function increases as k2 increases slightly. However, as the temperature continues to rise, a subtle decrease in the partition function is observed, indicating that at higher thermal energies, the system's sensitivity to changes in k2 becomes more complex.

Conclusion

This study examined the energy spectrum obtained from the non-relativistic Schrödinger equation by varying dimensionless potential parameters and applying different statistical distributions to assess their influence on molecular behaviour. It was found that lower dimensionless potential parameter values (V_0, V_1) generally lead to higher energy spectrum similar increase intermolecular behaviour, while increasing these parameters suppresses the energy spectrum and reduces the molecular behaviour. Across Maxwell-Boltzmann, Fermi-Dirac, Boltzmann, and Bose-Einstein distributions, temperature consistently broadens the energy distribution and elevates energy spectrum, though effects vary with the statistical model and dimensionless potential parameter settings. The partition function typically increases with temperature and lower k2 values but shows complex behaviour under stronger potentials. Overall, both dimensionless potential parameters and temperature play a critical role in shaping energy states and system behaviour.

References

Alrebdi, H. I., Ikot, A. N., Horchani, R., & Okorie, U. S. (2024). A non-relativistic 2D Quantum System and Its Thermo-Magnetic Properties with a Generalized Pseudo-Harmonic Oscillator. Mathematics, 12(17), 2623.

Dong, S. H. (2000). Exact solutions of the two-dimensional Schrödinger equation with certain central potentials. International Journal of Theoretical Physics, 39(4), 1119-1128.

Ettah, E. (2021). The Schrödinger Equation with Deng-Fan-Eckart Potential (DFEP): Nikiforov-Uvarov-Functional Analysis (NUFA) Method. European Journal of Applied Physics, 3(5), 58-62.

Ikot, A. N., Okorie, U. S., Amadi, P. O., Edet, C. O., Rampho, G. J., & Sever, R. (2021). The Nikiforov–Uvarov-Functional Analysis (NUFA) Method: A new approach for solving exponential-type potentials. Few-Body Systems, 62(1), 9.

M. Abu-Shady and E. M. Khokha, "A precise estimation for vibrational energies of diatomic molecules using the improved Rosen–Morse potential," Sci Rep, vol. 13, no. 1, Dec. 2023, doi: 10.1038/s41598-023-37888-2.

Manga, P. J., Amusat, R. O., Dibal, A. A., Adamu, A., & Ubale, S. A. (2025A). Estimation of Energy Eigenvalues using an Exponential Screened plus Yukawa Potential under the Influence of an External Magnetic Field. Journal of Science Research and Reviews, 2(3), 66-79.

Manga, P. J., Amusat, R. O., Teru, P. B., Dibal, A. A., Likta, W. E., Omolara, O. V., ... & Ubale, S. A. (2025C). Determination of Thermodynamic Properties via Partition Function Approaches Derived from the Non-Relativistic Schrödinger Equation. Nigerian Journal of Theoretical and Environmental Physics, 3(2), 42-59.

Manga, P. J., Amusat, R. O., Teru, P. B., Likta, E. W., Dibal, A. A., Yahaya, M. N., ... & Isyaku, S. (2025B). Computing energy fluctuations in diatomic molecules through thermodynamic properties using the partition function approach. Science World Journal, 20(2), 760-773.

Manga, P. J., Buteh, S. D., Maina, M., Amusat, R. O., Teru, P. B., Hashimu, M. U., & John, D. S. (2023). Solutions of Schrödinger equation based on Modified Exponential Screened Plus Yukawa Potential (MESPYP) within the frame of parametric Nikiforov-Uvarov method. Dutse Journal of Pure and Applied Sciences, 9(3b), 144-154.

Umirzakov, I. (2019). Incorrectness of analytical solution of Schrodinger equation for diatomic molecule with shifted Tietz-Wei potential. arXiv preprint arXiv:1902.04977.